Magnetic resonance imaging of head and neck vascular anomalies: pearls and pitfalls

Shaimaa Abdelsattar Mohammad[a], Amr Abdelhamid AbouZeid[b], Ahmed M. Fawzi[b], Mohamed M. Dahab[b], Iman A. Ragab[c] and Osama El-Naggar[b]

Purpose **The aim of this study was to describe typical MRI features of the head and neck vascular anomalies and the possible diagnostic pitfalls.**

Patients and methods **Patients with extracranial vascular anomalies of the head and neck, who underwent MRI examinations between January 2013 and January 2016, were included in the study. Precontrast and postcontrast T1-WI, T2-WI, with and without fat saturation were acquired. When indicated, a noncontrast MR angiography was performed. Dynamic postcontrast MRI techniques were available in six children.**

Results **The study included 33 patients (age ranged from 10 to 20 years, mean: 49 months). MRI confirmed the clinical diagnosis in equivocal cases, and provided proper determination of lesion extension and/or associated intracranial anomalies. The study included 10 cases of vascular tumors (hemangioma), whereas the remaining 23 cases had the diagnosis of vascular malformations (one patient with arteriovenous malformation, one with capillary malformation, seven with venous, nine with macrocystic lymphatic, and five with microcystic lymphatic malformations).**

Conclusion **Vascular anomalies in the head and neck are mostly diagnosed on clinical basis; however, when the history is uncertain or the diagnosis is equivocal, a well-tailored MR examination can be a single valuable diagnostic tool providing structural and functional information.** ***Ann Pediatr Surg*** **13:116–124 © 2017 Annals of Pediatric Surgery.**

Annals of Pediatric Surgery 2017, **13**:116–124

Keywords: children, head and neck, hemangioma, lymphatic malformation, magnetic resonance angiography, venous malformation

Departments of [a]Radiodiagnosis, [b]Pediatric Surgery and [c]Pediatrics, Faculty of Medicine, Ain-Shams University, Cairo, Egypt

Correspondence to Amr Abdelhamid AbouZeid, MD, Department of Pediatric Surgery, Faculty of Medicine, Ain-Shams University, Lotefy El-Sayed Street, 9 Ain-Shams University Buildings, Abbassia, Cairo 11657, Eygpt
Tel: +20 111 656 0566; fax: +20 224 830 833;
e-mail: amrabdelhamid@hotmail.com

Received 30 June 2016 **accepted** 4 February 2017

Introduction

Soft tissue vascular anomalies comprise a wide spectrum of abnormalities of the blood and lymphatic vessels. Management of affected persons has considerably improved over the last few years. This can be attributed to the adoption of a comprehensive binary classification system (dividing vascular anomalies into tumors and malformations on the basis of their clinicopathological features) [1], in addition to the establishment of multidisciplinary teams for managing the vascular anomalies in many institutions all over the world [2]. Among the vascular tumors, infantile hemangiomas represent the most common tumor of infancy; they have an anatomic predilection for the head and neck regions [3].

Accurate differentiation between vascular tumors (most commonly hemangiomas) and vascular malformations is crucial, as their management is completely different [4]. Most cases of vascular anomalies can be diagnosed by careful history and thorough physical examination. However, the role of imaging is not only to confirm the clinical diagnosis in equivocal and complex cases but also to determine the exact extension of the lesion before surgery or any other intervention. In addition, imaging can provide a useful tool for assessing the response to therapy in the follow-up of these cases [4]. Therefore, in most institutions, a well-experienced radiologist represents a key member in the multidisciplinary team for managing vascular anomalies.

Ultrasound and MRI are the two primary imaging techniques employed in the assessment of vascular anomalies. Ultrasound is widely available, easy to use, noninvasive, has low cost, and usually does not require sedation. However, the value of ultrasound may be limited in deep and complex lesions [5]. MRI has the advantage of superior soft tissue resolution enabling the assessment of the deep extension of the lesion, and the involvement of nearby structures in absence of ionizing radiation. Moreover, MRI has the advantage of providing data that can be easily shared by other radiologists and clinicians. Different MRI protocols have been adopted for imaging vascular anomalies. A multidisciplinary center recommended conventional T1-weighted imaging (T1-WI) spin-echo, fat-saturated T2-WI fast spin-echo, and flow-weighted sequences with no need for contrast administration [6]. Other researchers highlighted the role of contrast enhancement in the differentiation of venous from lymphatic malformations [7]. Thanks to its high temporal resolution, time-resolved MR angiography has been recently added to increase the diagnostic efficacy of the study [8].

The aim of this study is to describe the typical and discriminating MRI features of the common vascular anomalies (affecting the head and neck region), in referral to the different MRI techniques, to increase the diagnostic confidence when dealing with these cases.

Patients and methods

Patients with extracranial vascular anomalies of the head and neck, who underwent MRI examinations at our

1687-4137 © 2017 Annals of Pediatric Surgery DOI: 10.1097/01.XPS.0000513183.56919.bf

Table 1 **Distribution of 31 cases of vascular anomalies in the head and neck region, in addition to the typical magnetic resonance imaging features and the commonly encountered imaging pitfalls**

Type of Vascular anomaly	Number of cases	Site	Non-contrast MRI	Non-contrast MR arteriography	Post-contrast sequences	Dynamic MRI	Commonly encountered imaging pitfalls
Hemangioma	3 (Congenital) 7 (Infantile)	Left occipital (2 cases) Right cheek Bilateral parotid (beard) Left parotid Left orbit Right cheek Scalp Nape Segmental ophthalmic	Well localized soft tissue mass. Isointense on T1WI. Hyperintense on T2WI. Intra-lesional flow voids.	Demonstrate feeding and intra-lesional high flow vessels	Uniform avid post-contrast enhancement	Demonstrate early post-contrast enhancement in arterial phase	Presence of prominent arterial feeding vessels is similar to arterio-venous malformations; however, the latter is composed of serpingious vessels lacking a soft tissue mass.
Venous malformations	7	Right mandibular (2 cases) Right intra-masseter Oropharynx Left neck (trans-spatial) Right cheek Left orbit + cheek	Localized or trans-spatial lesions. Hypointense on T1WI. Hyperintense on T2WI. Phleboliths and occasional fluid levels.	No prominent arterial feeding vessels	Typically non-uniform post-contrast enhancement	Demonstrate gradual post-contrast enhancement in venous and delayed phases	1. Fluid levels may confuse with lymphatic malformation. 2. A 'more or less' uniform postcontrast enhancement may confuse with hemangioma.
Macrocystic lymphatic malformation	9	Right neck (4 cases) Right orbit (2 cases) Left orbit Left cheek Right parotid	Cystic lesion. Hypointense on T1WI. Hyperintense on T2WI. Fluid levels.	No prominent arterial feeding vessels	Marginal and septal post-contrast enhancement		Deviation from the typical MRI signal intensity (hyperintense in T1WI or hypointense in T2WI) due to intra-cystic hemorrhage or high protein content
Microcystic lymphatic malformation	5	Right parotid Bilateral parotid (beard) Left orbit Right cheek Tongue	Diffuse sheets of abnormal signal infiltrating into surrounding tissue planes.	No prominent arterial feeding vessels	Ill defined (if any) post-contrast enhancement		Anomalous dilated veins may be seen in close proximity to the lesion (2 cases)

Two cases are not included (one with arteriovenous and another with capillary malformation).
MRA, magnetic resonance arteriography; T1-WI, T1-weighted imaging.

Fig. 1

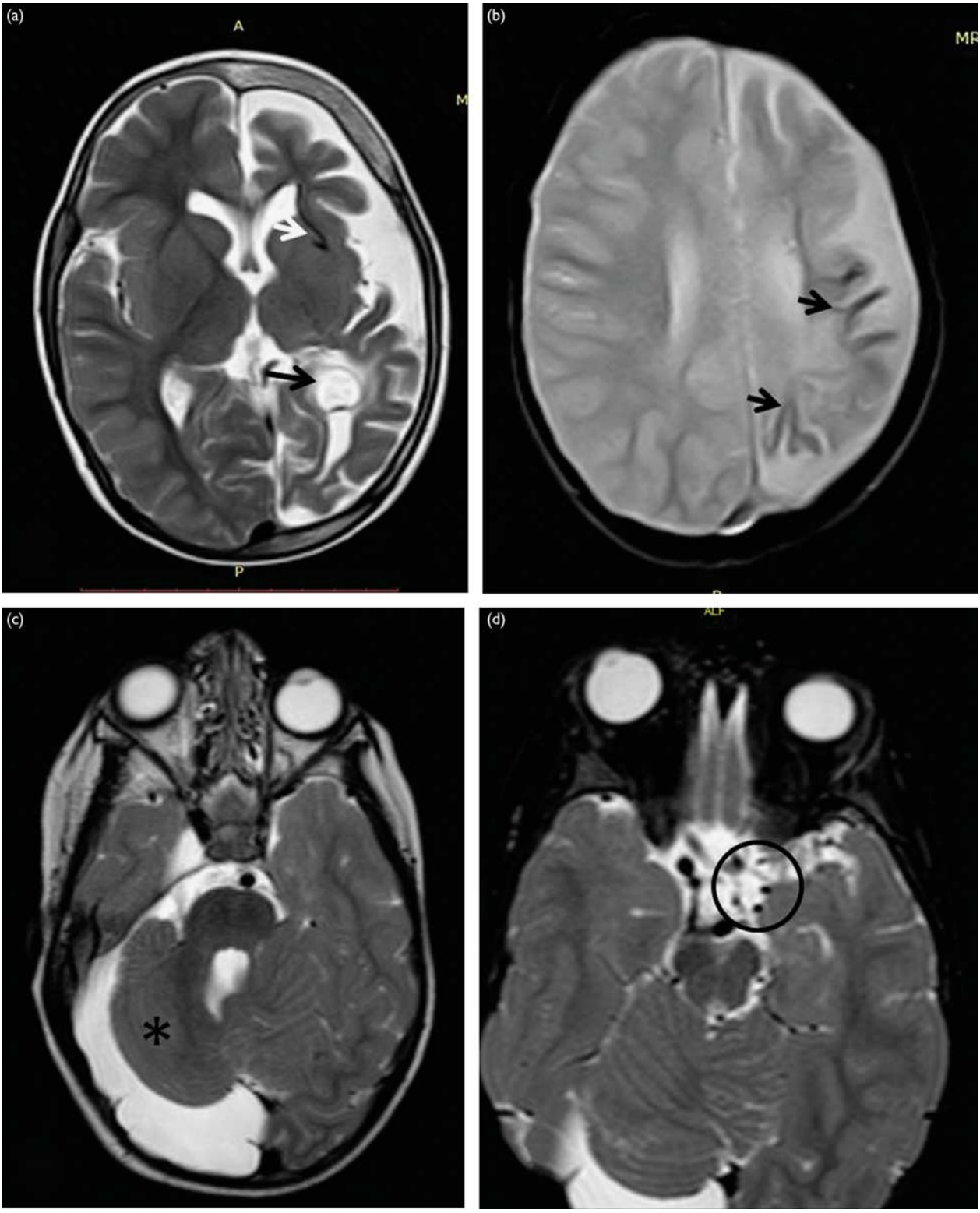

Syndromes associating vascular anomalies. (a, b) Five-year-old boy with Sturge–Weber syndrome (associating facial 'port wine' capillary malformation). (a) Axial T2-weighted imaging (T2-WI) shows left cerebral hemiatrophy, dilated deep veins (white arrow) with enlarged choroid plexus (black arrow); (b) axial T2* sequence shows gyral low-signal intensity consistent with gyral calcifications (black arrows). (c, d) Two-year old boy with PHACE syndrome (associating segmental facial infantile hemangioma). (c) Axial T2-WI with fat suppression showing right cerebellar hypoplasia (*) as a posterior fossa malformation; (d) axial T2-WI at a higher level reveals nonvisualization of the left internal carotid artery (circle).

institution between January 2013 and January 2016, were included in the study. Patients were referred for MRI examination either to confirm clinical diagnosis in equivocal cases or to define the deep extension of the lesion. Cases with segmental facial vascular anomalies were referred searching for associated intracranial abnormalities. The study was conducted after obtaining the approval of the internal review board.

Fig. 2

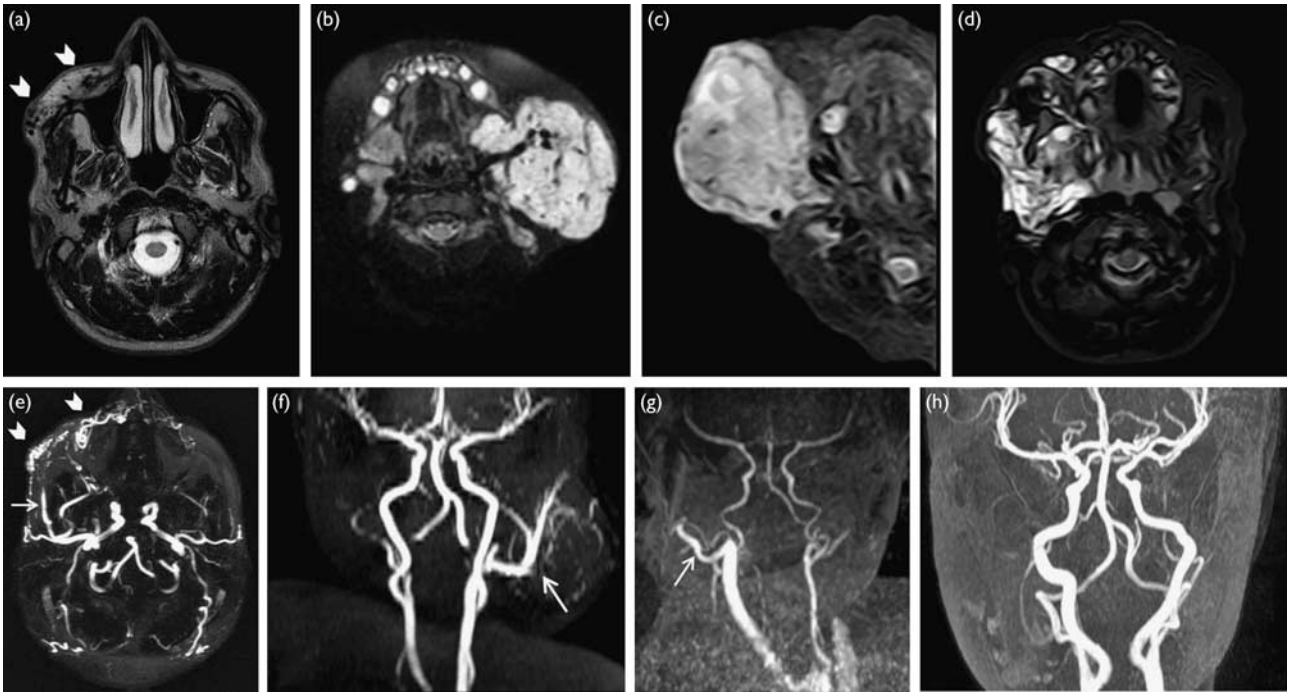

Role of noncontrast magnetic resonance arteriography (MRA) in differentiating high-flow from low-flow vascular anomalies. The upper row images (a–d) are axial T2-weighted imaging (T2-WI) of four different cases of vascular anomalies, and their corresponding noncontrast MRA (e–h) in the lower row. First case (a, e): 20-year-old patient with a 'high-flow' arteriovenous malformation (right cheek) demonstrating the high-flow vessels (arrowheads) that appear as flow voids in conventional T2-WI (a), and as serpiginous tubular structures without appreciable soft tissue component in MRA (e); note the presence of ipsilateral prominent feeding arteries (white arrow) in the MRA. Second case (b, f): 9-month-old girl with a 'high-flow' infantile hemangioma of the left parotid gland; note the prominent intralesional flow voids in (b) and the presence of ipsilateral prominent feeding arteries (white arrow) in the MRA (f). Third case (c, g): 15-day-old boy with a 'high-flow' congenital hemangioma of the right cheek demonstrating an ipsilateral prominent feeding artery (white arrow) in the MRA (g). Fourth case (d, h): 4-year-old girl with a 'low-flow' lymphatic malformation of the right parotid gland demonstrating the absence of related high-flow vessels in MRA (h).

Children under the age of 6 years were sedated by oral chloral hydrate. Performing the examination under general anesthesia was scheduled after failure of oral sedation. MRI examination was performed using a 1.5-T magnet with a 16-channel phased-array neurovascular coil. Axial T1-WI spin-echo (TR/TE/flip angle: 645/15 ms/90°); axial T2-WI fast spin-echo (TR/TE/flip angle: 5297/110 ms/90°); axial, sagittal, and coronal fat-saturated T2-WI fast spin-echo were acquired for all patients. When indicated, a noncontrast angiography multiple two-dimensional (M2D) inflow was performed in the axial plain (TR/TE/flip angle: 12/2.4 ms/60°) followed by maximum-intensity projection coronal reconstruction. A saturation slap was selected to suppress the venous flow signal. In most cases, additional fat-saturated T1-WI spin-echo was acquired in multiple planes following the injection of 0.1 mmol/kg gadopentetate-dimeglumine.

Dynamic postcontrast MRI techniques were available in six children. Dynamic T1 high-resolution isotropic volume examination (THRIVE) was available in four children, whereas 4D time-resolved angiography using keyhole (4D TRAK) was available in two. The 4D TRAK sequence is a 3D Turbo Field Echo resolution sequence containing 24 dynamics (TR/TE/flip angle: 3.1/1.2 ms/35°). Dynamics were acquired with a temporal resolution of 1 s for each phase. Dynamic THRIVE sequence had included six dynamics (TR/TE/flip angle: 3.9/1.8 ms/10°). The contrast material (gadopentetate-dimeglumine) was injected in a dose of 0.2 mmol/kg followed by the same volume of saline flush. Imaging postprocessing was performed to acquire time-intensity curves. Postcontrast fat-saturated T1-WI spin-echo images were acquired at the end of dynamic phases. All fat-saturated sequences were acquired using Spectral Adiabatic by Inversion Recovery.

Image analysis

The vascular anomalies were diagnosed as vascular tumors or vascular malformations following the previously described typical MRI features [5,7,9], and according to the classification proposed by Mulliken and Glowacki [1] in 1982 and its recent update of the International Society of Study of Vascular Anomalies (ISSVA) [10]. Differentiation between the different vascular lesions was made according to their signal intensity on T1-WI spin-echo, T2-WI fast spin-echo, and the pattern of postcontrast enhancement. The lesion extension was assessed in fat-saturated T2-WI fast spin-echo. In some cases, noncontrast magnetic resonance arteriography (MRA) and/or dynamic postcontrast sequences were also available for analysis.

Results

Thirty-three patients with different types of vascular anomalies were enrolled in this study. Table 1 demonstrates their distribution in the different regions of the head and neck. Their age ranged from 10 days to 20 years (mean: 49.3

Fig. 3

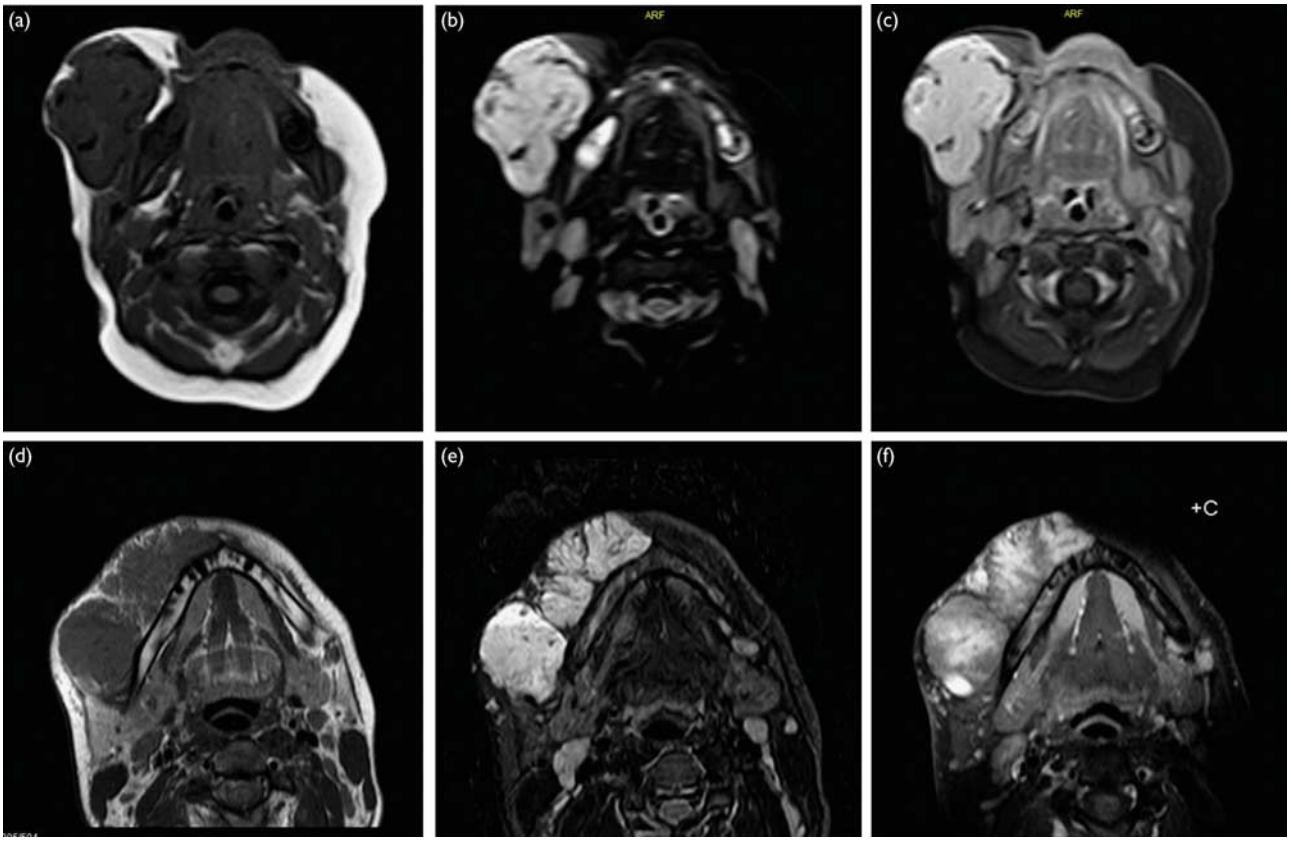

The upper row (a–c): MRI of a 7-month-old girl with infantile hemangioma (right cheek) showing isointense tumor parenchyma on T1 (a), hyperintense on T2 (b), and avid uniform enhancement on postcontrast fat-suppressed T2-weighted imaging (T1-WI) (c). The lower row (d–f): MRI of a 17-year-old patient with venous malformation (right mandibular region) showing hypointense signal on T1 (d), hyperintense on T2 (e), and patchy nonuniform enhancement on postcontrast fat-suppressed T1-WI (f).

months). MRI confirmed the clinical diagnosis in equivocal cases, and provided proper determination of lesion extension and/or associated intracranial anomalies (Fig. 1). The study included ten cases of vascular tumors (hemangioma), whereas the remaining 23 cases had the diagnosis of vascular malformations (one patient with arteriovenous malformation, one with capillary malformation, seven with venous, nine with macrocystic lymphatic, and five with microcystic lymphatic malformations). Arteriovenous malformation was demonstrated in one case as serpiginous high-flow vessels without appreciable soft tissue parenchyma (Fig. 2a and e). Another case with left facial 'port wine' capillary malformation was found to have associating intracranial abnormalities as a part of Sturge–Weber syndrome (Fig. 1a and b).

In our study group, cases of vascular tumors were either infantile hemangioma (seven cases) or congenital hemangioma (three cases). Conventional noncontrast MRI typically showed a well-localized soft tissue mass exhibiting isointense signal on T1-WI, hyperintense signal on T2-WI, with characteristic prominent equatorial flow voids (Figs 2b, c and 3a, b). Noncontrast MRA further increased the diagnostic confidence by demonstrating the high-flow feeding and intralesional vessels (Fig. 2). Postcontrast sequences (available in seven cases) showed the typical avid uniform enhancement (Fig. 3c). Postcontrast dynamic THRIVE was performed in one child and revealed arterial phase enhancement. Segmental facial infantile hemangioma appeared as cutaneous thickening in one patient who had associating intracranial abnormalities as a part of the Posterior fossa brain malformation, Hemangioma, Arterial lesions, Cardiac and Eye abnormalities (PHACE) syndrome (Fig. 1c and d).

Venous malformations (seven cases) appeared either as a localized lobulated mass (five cases) or a diffuse transpatial lesion (two cases). Postcontrast MRI sequences are usually needed for proper characterization of the vascular nature of the lesion (Fig. 3d–f). Gradual enhancement in the venous and delayed phases can be demonstrated by applying the more recent dynamic postcontrast MRI techniques (available in five cases) (Fig. 4). The presence of phleboliths was reported to be pathognomonic (Fig. 5a and b) [9], whereas fluid levels may confuse with macrocystic lymphatic malformation (Fig. 5c).

Fourteen cases of lymphatic malformation were included in the study (nine macrocystic and five microcystic) (Table 1). Typically, macrocystic lymphatic malformation appeared as well-defined multiloculated cystic mass exhibiting hypointense signal on T1-WI spin-echo, and hyperintense signal on T2-WI fast spin-echo (Fig. 6a–c). However, some of the locules exhibited the reverse (hyperintense signal on T1-WI spin-echo, or hypointense signal on T2-WI fast spin-echo) likely because of intracystic hemorrhage and/or high protein

Fig. 4

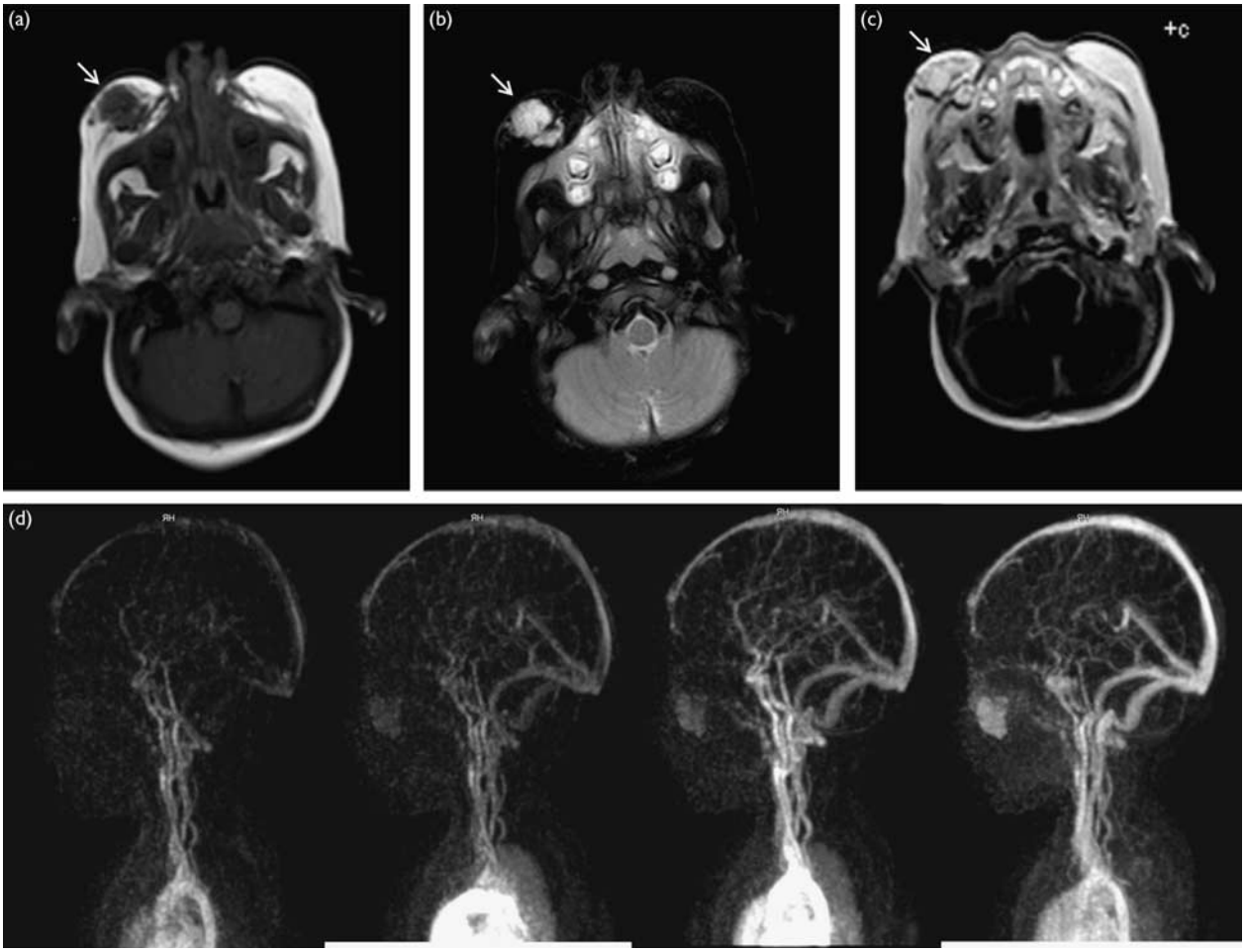

Six-month-old girl with a lump in the right cheek confirmed by MRI to be venous malformation. The lesion (arrow) is demonstrating hypointense signal on T1 (a), hyperintense on T2 (b), and a 'more or less' uniform enhancement on postcontrast T2-weighted imaging (T1-WI) (c) that might be confused with hemangioma. (d) Sagittal maximum-intensity projection four-dimensional time-resolved angiography using keyhole reveals absence of early enhancement in the arterial phase, with gradual enhancement during the venous phase of the study, confirming its venous nature.

Fig. 5

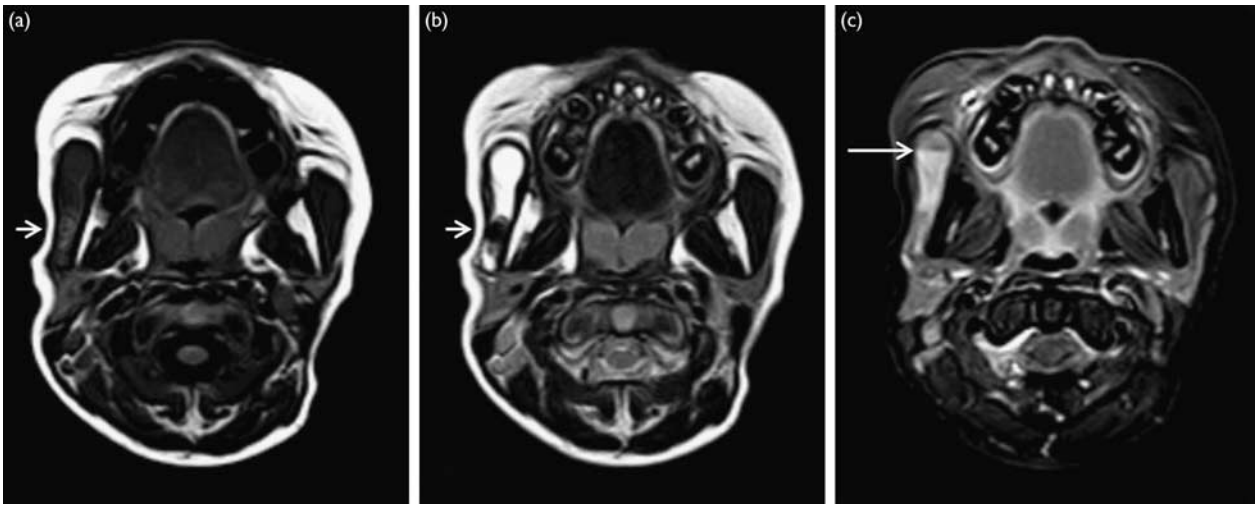

MRI of a 6-month-old girl with venous malformation (right intramasseter) showing hypointense signal on T1 (a), hyperintense on T2 (b), and postcontrast enhancement on fat-suppressed T1-weighted imaging (c). Note the presence of phleboliths (short arrow) and a fluid level (long arrow), which indicates stasis of the blood within the venous channels.

Fig. 6

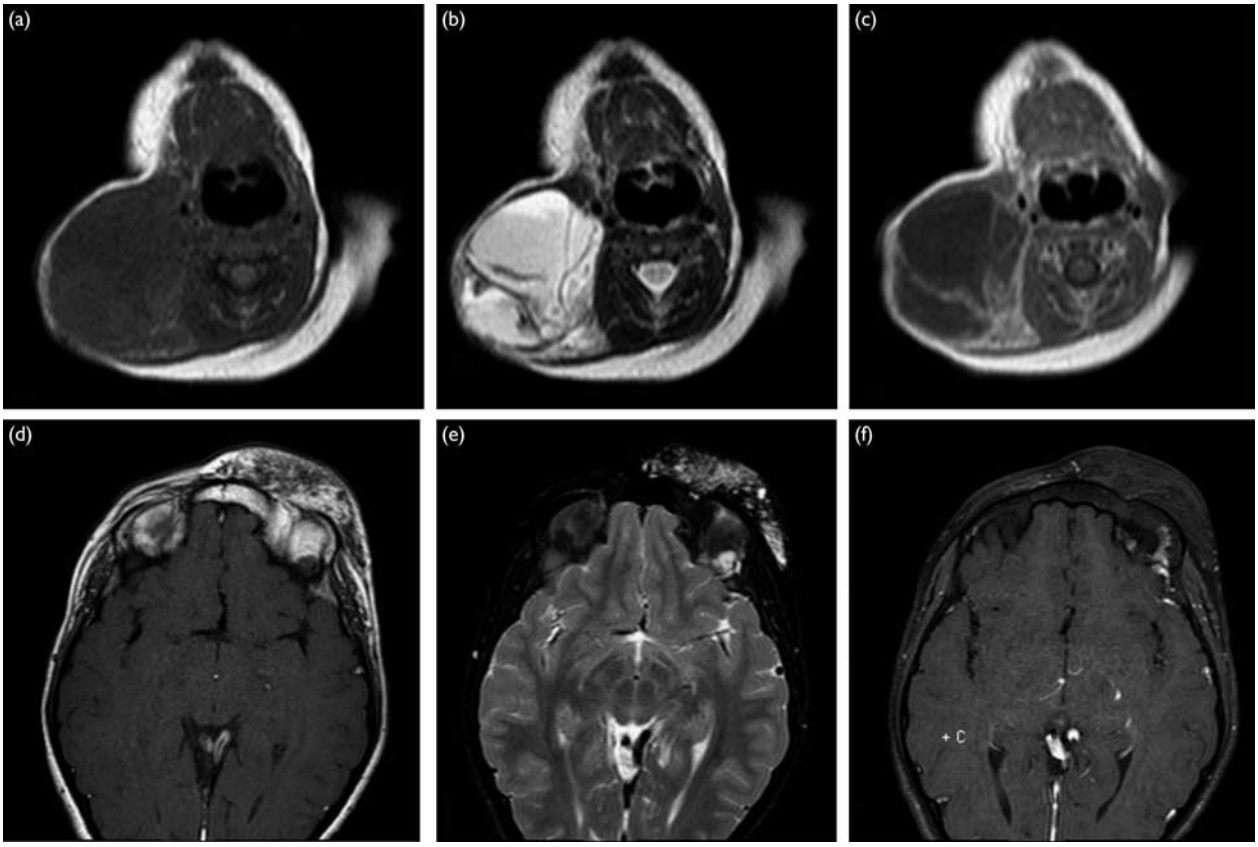

The upper row (a–c): MRI of a 2-month-old boy with macrocystic lymphatic malformation (neck) showing hypointense signal on T1 (a), hyperintense on T2 (b), and characteristic marginal and septal enhancement on postcontrast T1 (c). The lower row (d–f): MRI of a 15-year-old girl with microcystic lymphatic malformation (left orbit) demonstrating the lesion as sheets of abnormal intensity (hypointense on T1 and hyperintense on T2), with absence of enhancement on postcontrast fat-suppressed T1 (f).

content (Fig. 7). Characteristically, macrocystic lymphatic malformation showed marginal and septal contrast enhancement of the cystic spaces (Fig. 6c), in addition to fluid levels (Fig. 7). Microcystic lymphatic malformation appeared as diffuse sheets of abnormal signal with no appreciable contrast enhancement (Fig. 6d–f).

Discussion

Despite the widely accepted classification system of vascular anomalies, the indiscriminate application of the term hemangioma to different vascular anomalies (ignoring their different pathophysiologies) has led to dissemination of faulty information to patients and clinicians, and has increased the confusion in diagnosing and treating these lesions. Understanding the clinicopathological and radiological differences between vascular tumors and vascular malformations is crucial in designing a suitable treatment plan [2].

Infantile hemangiomas are the most frequent vascular tumors, and are most often found in the head and neck. They have proliferative phase during early infancy (high-flow lesions), and then involute by fibrofatty replacement by adolescence. In contrast, congenital hemangiomas are less common, and are fully developed at birth. Hemangiomas can present as superficial dermal lesions when the diagnosis is easily made on clinical basis (with no need for further investigations). However, the diagnosis of deeper hemangiomas with normal overlying skin can be challenging [4]. Among the head and neck regions, hemangiomas of the orbit and beard distribution are considered alarming hemangiomas that require imaging to define their deep extension (possible visual problems and airway compromise, respectively) [11]. Kaposiform hemangioendothelioma typically presents at birth (most often involves the trunk, extremities, and retroperitoneum), and extends across tissue planes [10]. It is categorized as borderline or locally aggressive tumor [10].

Vascular malformations are usually apparent at birth and grow proportionally with the growth of the child. They are divided into high-flow (arteriovenous) and low-flow malformations (venous, lymphatic, and capillary). Arteriovenous malformations are less common but probably the most challenging to treat [5]. Venous malformations are more common with 40–60% of cases encountered in the head and neck region [12], whereas 74% of lymphatic malformations are located in the neck [12]. Vascular malformations can be focal or infiltrative (extending through tissue planes). They are usually diagnosed clinically. Imaging is reserved for atypical cases and to define the deep extension of the lesion before surgery or imaging-guided intervention.

Segmental facial vascular anomalies can be an indicator of one of the two famous neurocutaneous syndromes: Sturge–Weber

Fig. 7

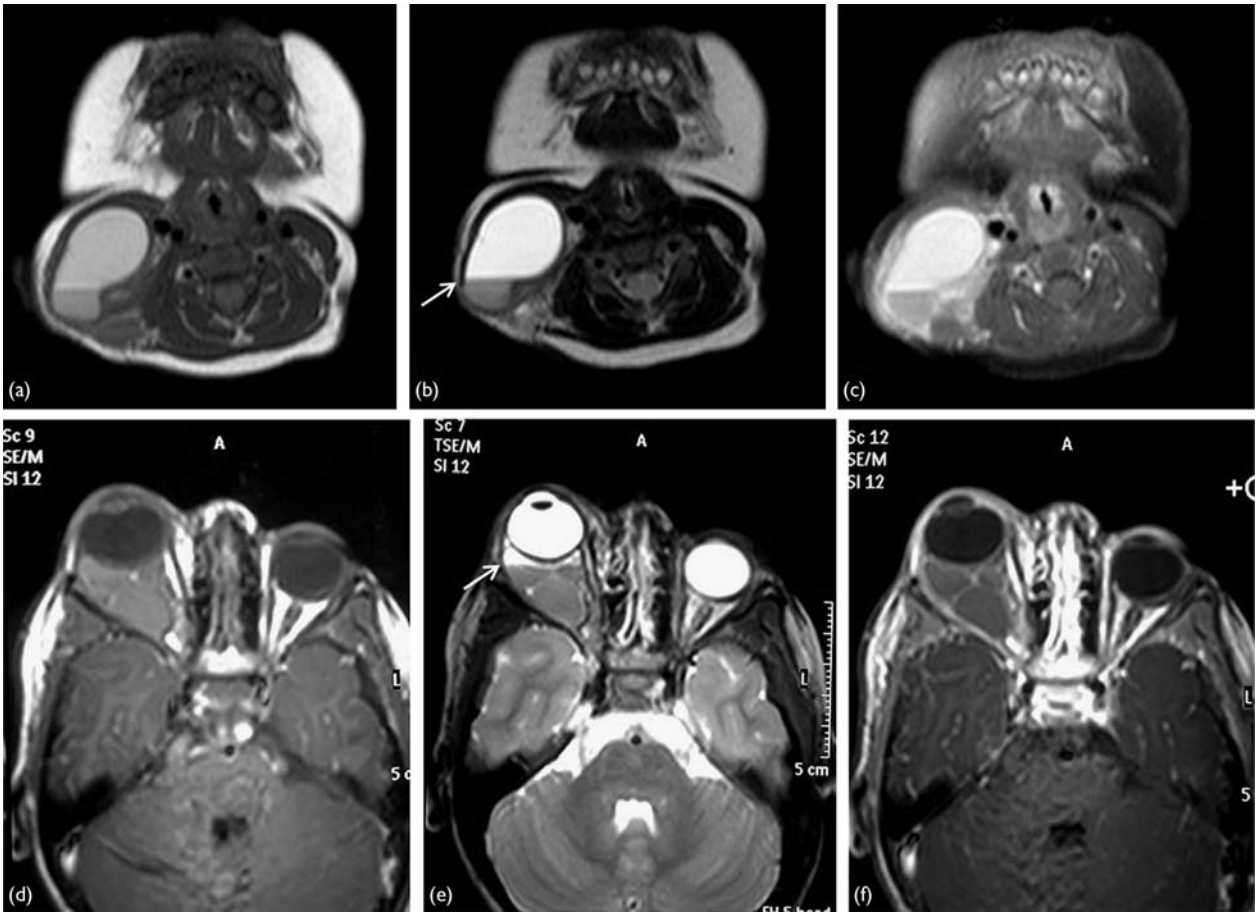

The upper row (a–c): MRI of a 5-month-old boy with macrocystic lymphatic malformation (neck) showing 'atypical' predominant hyperintense signal on T1 (a), hyperintense signal on T2 (b), and postcontrast marginal enhancement (c); note the presence of characteristic fluid level. The lower row (d–f): MRI of a 5-year-old girl with macrocystic lymphatic malformation (right orbit) showing hypointense signal on T1 (d), 'atypical' predominant hypointense signal on T2 (e), and postcontrast marginal enhancement (f). The presence of atypical MRI intensity in cases of lymphatic malformations can be attributed to the presence of intracystic hemorrhage or high protein content of the intracystic fluid.

and PHACE syndromes. MRI is the modality of choice to detect the associating intracranial abnormalities. Sturge–Weber syndrome is characterized by facial capillary malformation in the distribution of ophthalmic branch of the trigeminal nerve in association with leptomeningeal angiomatosis and choroidal angioma [13]. PHACE syndrome is a neurocutaneous syndrome of posterior fossa malformation, segmental hemangioma, coarctation of the aorta, cardiac, and eye abnormalities. The hallmark of PHACE syndrome is a large segmental hemangioma of trigeminal dermatome pattern [14].

MRI has been introduced as a superior modality for studying vascular anomalies, owing to its multiplanar capabilities, high soft tissue resolution, and absence of ionizing radiation. Apart from arteriovenous malformations, which appear as multiple serpiginous vessels with no considerable soft tissue component [5–7], most vascular tumors and malformations demonstrate soft tissue masses with similar hypointense signal on T1-WI and hyperintense signal on T2-WI. The extent of the lesion can be well demonstrated in the conventional MRI sequences (fat-saturated T2-WI); however, when the clinical diagnosis is equivocal, the pattern of postcontrast enhancement helps in the differentiation between different types of vascular anomalies. Macrocystic lymphatic malformations have a characteristic marginal enhancement of the cystic spaces, whereas venous malformations typically demonstrate a patchy pattern of enhancement compared with the avid uniform enhancement of hemangiomas [9]. Minimal, if any, enhancement is seen in cases of microcystic lymphatic malformations. Contrast-enhanced sequences can be challenging in children because of difficulties in obtaining suitable intravenous access. Furthermore, contrast injection can be prohibited in certain situations, especially in neonates with immature kidneys or children with impaired renal function when the benefit of contrast injection does not outweigh the possible risk for nephrogenic systemic fibrosis. In addition, performing MRI examination without contrast injection reduces the cost and decreases the timing of examination, especially in children under sedation.

Noncontrast MRA can confirm the diagnosis of high-flow lesions (arteriovenous malformations and noninvoluted hemangiomas) by demonstrating their high-flow feeding and intralesional vessels. Inflow MR Technique is based on the enhancement of the moving blood with suppression of stationary tissues [15]. It can be applied as M2D or 3D acquisition. M2D MRA is well suited to cover a large track of a vessels, which makes it suitable for imaging the relatively straight carotid vessels [15]. Moreover, it is performed with

no contrast administration making this technique suitable for patients not tolerating gadolinium contrast. However, this technique fails to provide the detailed hemodynamic characteristics of other vascular anomalies. Recently dynamic postcontrast MR sequences (either 4D TRAK, or THRIVE) have been added to the imaging protocol of vascular anomalies for detailed demonstration of their functional and hemodynamic behavior [8]. The 4D TRAK has the advantage of higher temporal resolution allowing examination of the lesion during arterial, capillary, and venous phases [8]. Dynamic THRIVE sequence has the advantage of high spatial resolution allowing good depiction of the vascular structures and the surrounding soft tissues.

Occasionally, the differentiation between hemangiomas and venous malformations can be challenging, both clinically and radiologically. Presence of high-flow vessels is the main determinant of noninvoluted hemangiomas. High-flow vessels can be depicted as flow voids on conventional MR sequences. However, the presence of hypointense fibrous striation or dilated veins in cases of venous malformations can be falsely interpreted as flow voids of high-flow vascular tumors [8]. Moreover, venous malformation can demonstrate uniform postcontrast enhancement similar to hemangioma, and phleboliths can be found occasionally in hemangioma [8]. In such cases, noncontrast MRA will clearly demonstrate the high-flow feeding and intralesional vessels in hemangiomas, but not with venous malformations. In addition, the 4D TRAK or dynamic THRIVE can be superior in differentiating venous malformation from hemangiomas [8]. Hemangiomas show early arterial enhancement, whereas venous malformations remain unenhanced in the arterial phase and show gradual delayed enhancement during the venous phase (Fig. 4).

This study was limited by the relatively small number of cases, in addition to the absence of pathological correlation. However, we were strictly following the previously described characteristic MRI features of vascular tumors and malformations, and in selected cases we complemented the study by MRA and dynamic MRI sequences to increase the diagnostic confidence by demonstrating the detailed hemodynamic characteristics of the lesion. Less frequent types of vascular tumors (tufted angioma and sarcoma) were not encountered in this study; however, a variety of common vascular anomalies in the head and neck were clearly illustrated, stressing on the similarities, the differentiating points, and the potential diagnostic pitfalls, in relation to the different MRI techniques.

Conclusion

Vascular anomalies in the head and neck are mostly diagnosed on clinical basis; however, when the history is uncertain or the diagnosis is equivocal, a well-tailored MR examination can be a single valuable diagnostic tool providing structural and functional information. Knowing the typical imaging features and potential pitfalls is crucial to avoid the misinterpretation and faulty diagnosis.

Acknowledgements

Part of this work has been accepted as electronic poster (EPOS) at European Congress of Radiology (ECR) 2016.

Conflicts of interest

There are no conflicts of interest.

References

1 Mulliken JB, Glowacki J. Hemangiomas and vascular malformations in infants and children: a classification based on endothelial characteristics. *Plast Reconstr Surg* 1982; **69**:412–422.
2 Adams DM, Lucky AW. Cervicofacial vascular anomalies. Hemangiomas and other benign vascular tumors. *Semin Pediatr Surg* 2006; **15**:124–132.
3 Haggstrom AN, Drolet BA, Baselga E, Chamlin SL, Garzon MC, Horii KA, *et al*. Prospective study of infantile hemangiomas: demographic, prenatal, and perinatal characteristics. *J Pediatr* 2007; **150**:291–294.
4 Dubois J, Alison M. Vascular anomalies: what a radiologist needs to know. *Pediatr Radiol* 2010; **40**:895–905.
5 John P. Vascular anomalies. In: Temple M, Marshalleh FE, editors. *Pediatric interventional radiology: hand book of vascular and non-vascular interventions*. New York: Springer; 2014. pp. 177–224.
6 Donnelly LF, Adams DM, Bisset GS. Vascular malformations and hemangiomas: a practical approach in a multidisciplinary clinic. *Am J Roentgenol* 2000; **174**:597–608.
7 Meyer JS, Hoffer FA, Barnes PD, Mulliken JB. Biological classification of soft-tissue vascular anomalies: MR correlation. *Am J Roentgenol* 1991; **157**:559–564.
8 Kim JS, Chandler A, Borzykowski R, Thornhill B, Taragin BH. Maximizing time-resolved MRA for differentiation of hemangiomas, vascular malformations and vascularized tumors. *Pediatr Radiol* 2012; **42**:775–784.
9 Flors L, Leiva-Salinas C, Maged IM, Norton PT, Matsumoto AH, Angle JF, *et al*. MR imaging of soft-tissue vascular malformations: diagnosis, classification, and therapy follow-up. *Radiographics* 2011; **31**:1321–1340.
10 International Society of Study of Vascular Anomalies (ISSVA). Classification of Vascular Anomalies; 2014. Available at: *www.issva.org/classification*. [Accessed January 2016].
11 Restrepo R, Palani R, Cervantes LF, Duarte AM, Amjad I, Altman NR. Hemangiomas revisited: the useful, the unusual and the new. Part 2: endangering hemangiomas and treatment. *Pediatr Radiol* 2011; **41**:905–915.
12 Dompmartin A, Vikkula M, Boon LM. Venous malformation: update on aetiopathogenesis, diagnosis and management. *Phlebology* 2010; **25**:224–235.
13 Wasenko JJ, Rosenbloom SA, Duchesneau PM, Lanzieri CF, Weinstein MA. The Sturge-Weber syndrome: comparison of MR and CT characteristics. *Am J Neuroradiol* 1990; **11**:131–134.
14 Metry D, Heyer G, Hess C, Garzon M, Haggstrom A, Frommelt P, *et al*. Consensus statement on diagnostic criteria for PHACE syndrome. *Pediatrics* 2009; **124**:1447–1456.
15 Saloner D. An introduction to MR angiography. *Radiographics* 1995; **15**:453–465.